

Observations of Small-Separation Red Dwarf Binary Pairs Using Bispectrum Phase Reconstruction

Nathaniel Bowers,¹ Christine Filipek,² Nathan Lehenbauer,⁸ Mark McCarthy,³
Rinisha Ramprakash,⁴ Aparna Balaji,⁵ Kate North,⁶ Chloe Pendergrass,⁷
Ramprakash Surulirajan,⁹ Jayant Bhalerao¹⁰ Sierra Kasl-Goldey,¹¹
Jeffery Marx,¹² Anthony Maletta¹³ Jake North⁶, Supriya Roy⁶,
Ivan Altunin,¹⁴ Amber Mistry¹⁵

¹ Gettysburg College, natebowersnc@gmail.com

² REACH Tutorial

³ TriValley Stargazers

⁴ University of Georgia at Athens,

⁵ Centennial High School,

⁶ Stanford Online High School,

⁷ Loomis Chaffee High School,

⁸ San Diego Miramar College

⁹ Atlanta, GA

¹⁰ Dallas College

¹¹ Castro Valley High School

¹² McDaniel College

¹³ Harford Astronomical Society

¹⁴ University of California Berkeley

¹⁵ Georgia Institute of Technology

Abstract

Astrometric and photometric observations of eight potential late K and M red dwarf binary star systems within 100 parsecs of Earth were made using Sloan r' and i' filters. Observations were made in June 2021 using remote access of the Boyce Astro Robotic Observatory's telescope located outside of San Diego, CA. Observations consisted of 500-1000 images with exposures from 0.01 and 1 seconds. Speckle interferometry and bispectrum phase reconstruction allowed several hundred images to be combined to remove atmospheric noise and provide images suitable for astrometry. Methods and results are presented and discussed for each system. Our goal was to determine if the systems observed were physical binaries and to test the limits of the BARO telescope.

1. Introduction

Red dwarf binary pairs are of particular interest to astronomical research. Red dwarfs, characterized as late K or M spectral type stars, are the most common type of star (Henry et al. 2006). Despite their prevalence, we know comparatively little about red dwarfs due primarily to their size—typically only a few times larger than Jupiter—and their faintness. Consequently, red dwarfs have a low luminosity and are far more difficult to observe than other main sequence stars (Edgeworth 1946). Current red dwarf research aims to understand

their characteristics and formation. Further understanding of red dwarfs also assists the RECONS¹ mission to find every star within 25 parsecs of the sun (Henry et al. 2004).

Double stars fall into two categories. Optical double stars simply appear close when observed from Earth, but do not orbit each other. Physical double stars, also known as binary pairs, consist of a secondary star (by convention the less bright of the two) and a primary star (the brighter star) which revolve around a common barycenter. The fractions of stellar systems that are a binary pair vary with spectral type, and the stellar multiplicity rate is estimated to be $26 \pm 3\%$ for M type dwarfs and very similar for G and K dwarfs (Delfosse et al. 2004, Lada 2006). The orbital mechanics of double star systems can be solved for each component star, allowing for the mass of each component star to be found. Furthermore, binary systems, similar to red dwarfs, are crucial to finding and cataloging all nearby stars.

One method used to determine if a double star system is a binary pair—as opposed to an optical double or common motion pair—consists of observing the separation (ρ) and position angle (θ) between the two stars over time. If an elliptical orbit is observed, then it is likely that the two stars are gravitationally bound; if not, then it is unlikely. Double stars, however, tend to be difficult to observe due to the small separation between the two stars. At distances under the Rayleigh limit—a function of the diameter of the telescope and wavelength of light observed—the two stars visually merge to form an Airy disk. Atmospheric diffraction and turbulence further complicate the issue by introducing random noise and pushing observing limits above the theoretical Rayleigh limit.

Speckle interferometry is an imaging processing technique widely used to bypass this limit and observe double stars with a small separation angle (Dainty 1981; Morgan et al. 1978). Air pockets of different temperatures move and affect long exposure images by creating speckles while atmospheric movement is effectively zero for short exposure images. The primary and secondary stars will be affected in identical ways by the atmosphere, so information about the location of each star can be extracted via a Fourier transform over the sum of frequencies of observed positions (Dainty 1975). However, traditional interferometry cannot produce suitable images for astrometry due to the loss of phase data. Bispectrum phase reconstruction provides a workaround by extracting phase data from third-order moments of the Fourier transform (Petropulu & Nikias 1992). Through this relatively recent mathematical advance, precise astrometry on small separation binary pairs is possible.

Recent data releases from the European Space Agency's Gaia spacecraft have provided new data on potential red dwarf binaries and the discovery of hundreds of binary pairs (Jiménez-Esteban et al. 2019, Wasson et al. 2020). As part of its mission² to chart the Milky Way, the European spacecraft has provided precise astrometric data on over a billion objects. Using the Gaia data as a starting point, we found eight potential Red Dwarf binary pairs to observe and analyze using speckle interferometry and bispectrum phase reconstruction.

2. Methods

2.1 Equipment Used

The Boyce Astro Robotic Observatory's (BARO) telescope, located forty miles east of San Diego, CA, was used for observing. The telescope's primary mirror is 432 mm and its effective focal length is 2939 mm, giving it an effective focal ratio of f/6.8. Observations were made with Sloan r' and i' filters and a ZWO

¹ <http://www.recons.org/>

² <https://sci.esa.int/web/gaia>

ASI1600 CMOS camera. The theoretical Rayleigh limit of BARO is 0.366 arcseconds for the r' filter and 0.410 arcseconds for the i' filter.

2.2 Target Selection

Using the GAIA Double Star Selection Tool (GDS) developed by David Rowe to find potential double stars from the Gaia Data Release 2 (Gaia DR2), we found 747 stars that met our observation criteria. The baseline criteria were a right ascension between 14 and 19 hours and declination between -20 and 50 degrees—the range of the BARO telescope at the time of observation. Next, we limited the search to pairs where each star had an apparent G-magnitude between 6 and 12, Δmag was less than 2, and a separation angle between 0.5 and 2 arcseconds.

A color index (BMR) was formed by subtracting the R-magnitude from the B-magnitude for each star. A larger positive BMR then corresponds to a redder star; a small or negative value means it is bluer. For the first three stars, we only considered stars where both the primary and secondary had a $\text{BMR} > 1.8$. Only nine of the 747 binary pairs met these criteria. From those nine, we chose the three with the lowest gravitationally bound index (GBI) (Targets 1-3 in Table 1). This parameter is a very rough estimate of the likelihood of the stars being gravitationally bound (Rowe 2020, GDS Notes).

To pick the next three stars, we only considered the bright stars (6-8 mag primary) from the 747 potential targets. We further constrained the bright candidates by only considering pairs where both stars had a $\text{BRM} > 1$ to ensure red targets. From the seven remaining stars, we chose the brightest three (Targets 4-6 in Table 1). The final two stars were selected separately from the first three to have a low GBI. (Targets 7-8 in Table 1).

The primary motivation behind selecting these eight targets was to find likely red dwarf binary pairs. This dictated the use of a small separation angle, large BMR, and low GBI as selection criteria. A secondary motive was testing the capabilities of BARO. According to this goal, stars with a range of magnitudes and separation angles were selected.

Num	RA	Dec	GMag0	Gmag1	BMR0	BMR1	WDS
1	18:21:21	-09:14:49	11.486	11.784	2.106	2.085	N/A
2	18:21:01	-13:20:40	10.722	10.797	2.025	1.972	N/A
3	15:17:47	-09:22:11	11.379	11.809	1.906	1.97	N/A
4	18:25:18	48:45:42	7.468	7.779	1.067	1.049	18253+4846AC
5	14:41:45	09:31:40	8.067	8.107	1.088	1.164	14417+0932AB
6	14:31:20	-15:38:26	8.170	8.993	1.095	1.103	14313-1538AB
7	18:31:25	-1:28:20	11.279	11.318	1.91	2.061	N/A
8	17:57:03	15:46:39	11.789	11.854	2.544	2.604	17571+1547

Table 1. The six potential binary pairs found from Gaia DR2. RA and Dec refer to the position of the primary star. WDS name included for targets in the WDS catalog.

2.3 Observing

The eight potential binary pairs were observed in late June and early July of 2021, epoch 2021.4x. The faint targets (1-3) were hard to observe with an exposure time in the millisecond range, so a longer exposure was

necessary. This was not necessary with the brighter targets (4-6), so observations were significantly shorter. Each observation contained 500-1000 images.

Num	target i'	target r'	comp i'	comp r'	date
1	1.000	1.000	1.000	1.000	2021.47
2	1.250	0.350	0.080	0.050	2021.48
3	0.500	0.300	1.000	0.500	2021.47
4	0.020	0.020	0.050	0.050	2021.47
5	0.010	0.010	0.050	0.050	2021.47
6	0.050	0.020	0.010	0.010	2021.48
7	0.120	0.120	0.120	0.120	2021.49
8	0.300	0.300	0.050	0.050	2021.50

Table 2: Exposure time for each target and comparison star in each filter along with the date of observation. Exposure time is measured in seconds.

2.4 Historical Data

Alongside data from Gaia DR2 and our observations, other historical data was used for data processing and to potentially find trends in orbital data. The Washington Double Star Catalog (WDS) was used for historical data for targets 4-6. Data on the RA and Dec of each star was gathered from the Gaia Early Data Release 3 (Gaia EDR3). From the position data, separation (ρ) and position angle (θ) from EDR3 were calculated with formulas (1) and (2) respectively.

$$\rho = \arccos(\cos(\Delta RA)\cos(Dec0)\cos(\Delta Dec)) \quad (1)$$

$$\theta = \frac{\pi}{2} - \arctan\left(\frac{\sin(\Delta Dec)}{\cos(\Delta Dec)\sin(\Delta RA \cdot \cos(Dec0))}\right) \quad (2)$$

Where Dec0 is the declination of the primary star, ΔRA is the difference in right ascension between the secondary and primary star, ΔDec is the difference in declination between the secondary and primary star, and RA, Dec, ρ , and θ are measured in radians (Smolinski & Osborn 2006).

3. Data Analysis

3.1 Bispectrum Phase Reconstruction

For this paper, we used the program Speckle Toolbox (STB) to analyze our observations and perform astrometry. STB is a multi-purpose data reduction program developed by Dave Rowe that is particularly suited for measuring double stars (Harshaw et al. 2017). Each observation contained 500 to 1000 images of both the target binary and a comparison star. We performed bispectrum phase reconstruction to reduce our data and visually show the double star, and then we measured the separation and position angle with built-in astrometry tools. See Figure 1 for the bispectrum phase reconstruction and astrometry for each observation in both the r' and i' filter.

For some targets and filters, we were unable to resolve the data with STB. The two factors which determined if a target could be resolved are the separation angle and apparent magnitude. As the separation

angle approaches the Rayleigh limit, it becomes harder to resolve a target. From historic data, targets 2 and 5 have the smallest separation angle, and the difficulty in resolving them is apparent in Figure 1. Similarly, the dimmer stars necessarily had a longer exposure time, so bispectrum phase reconstruction is not as effective. This is also reflected in Figure 1. Furthermore, the Rayleigh limit is higher for the i' filter which helps explain why observations in the i' filter were harder to resolve.

3.2 Astrometry

After using bispectrum phase reconstruction in STB to analyze each target, we used the astrometry tool in STB to determine the separation and position angle of the pair. Each of the authors analyzed several targets with STB and measured the separation and position angle. For each target, the measurements across filters and authors were averaged and recorded in Table 3. There is no astrometric data for Target 2 since we were unable to resolve it.

Num	DR2 ρ	EDR3 ρ	Us ρ	DR2 θ	EDR3 θ	Us θ
Epoch	2015.5	2016.5	2021.47	2015.5	2016.5	2021.47
1	1.765	1.765	1.779	71.066	71.054	71.278
2	0.822	0.830	N/A	100.528	99.812	N/A
3	1.679	1.676	1.800	57.858	57.823	56.750
4	0.807	0.819	0.958	26.345	26.965	25.718
5	0.733	0.747	0.770	23.872	23.927	27.090
6	1.463	1.458	1.379	73.306	73.222	71.470
7	1.533	1.531	1.618	185.229	185.421	189.365
8	1.207	N/A	1.439	281.58	N/A	282.584

Table 3: Measurements of separation (ρ , arcseconds), position angle (θ , degrees), and the epoch of each measurement. Us refers to our observations while DR2 and EDR3 refer to the Gaia Data Release 2 and Early Data Release 3 respectively. We were unable to locate target 8 in the EDR3 catalog.

3.3 Parallax and historical trend analysis

To further evaluate whether the selected double stars are gravitationally bound, parallax, weighted separation, stellar mass, and the historical measurement trends were analyzed. The EDR3 parallax values were entered into a spreadsheet provided by Nathan Lehenbauer (Distance and Probability Calculator, DPC) which outputs the probability the two stars are within 1 light year of each other in the linear direction; the greater the probability percentage, the greater the probability the two stars are close enough together to be gravitationally bound.

An analysis of historical data was conducted by plotting both our measurements and historical measurements provided by the WDS using a Double Star Plot Tool (DSPT) provided by Ivan Altunin. The measurements taken during this study are shown as red triangles, and we evaluate whether our measures agree with historical trends. In cases where the star is not listed in the WDS, we plot three data points: the ρ and θ as calculated using equations (1) and (2) for DR2 (epoch 2015.5), EDR3 (2016.5), and our measurements (2021.4x).

1 2021-06-23 r' | 1 2021-06-23 i' | 2 2021-06-27 r' | 2 2021-06-27 i'

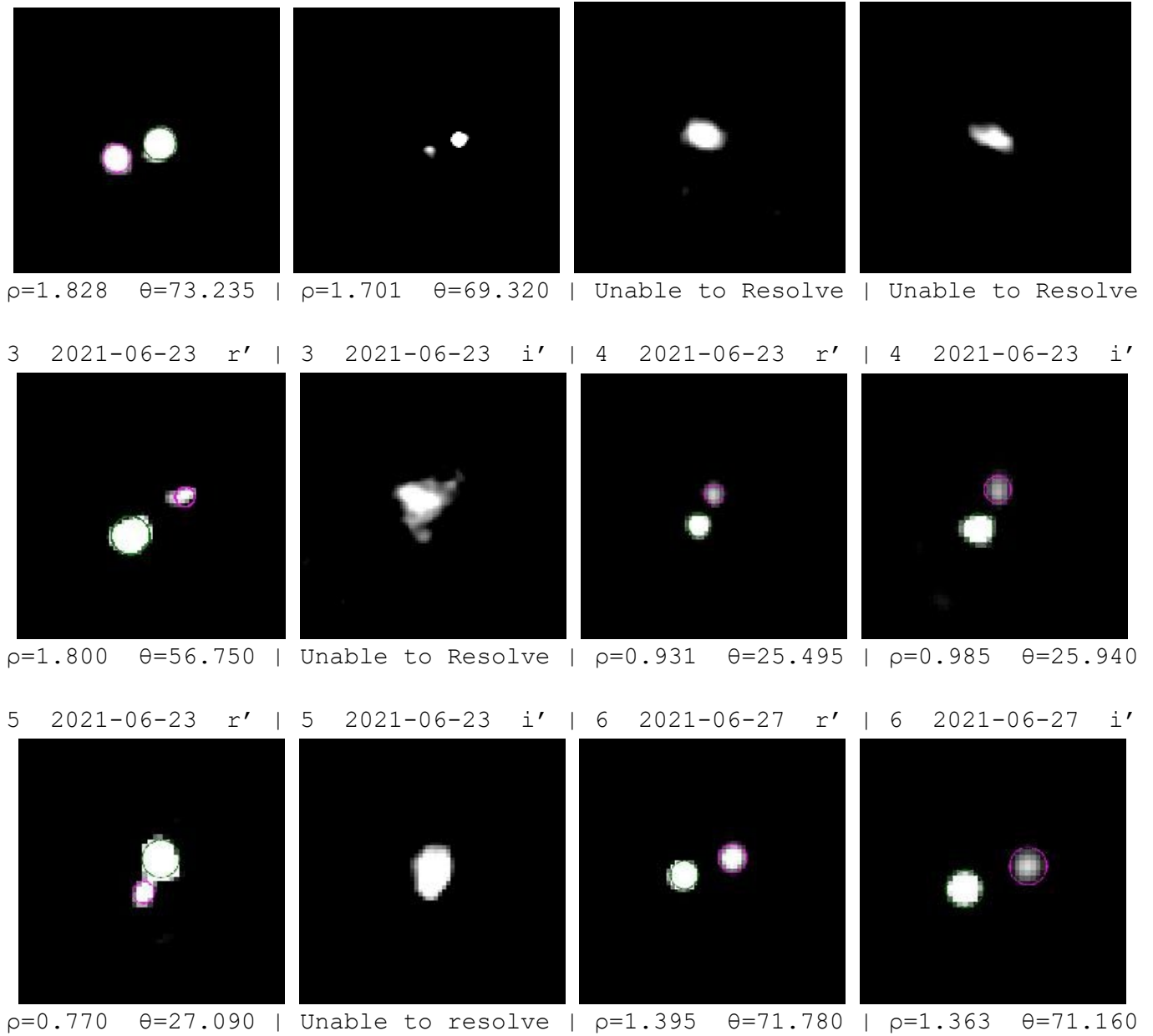
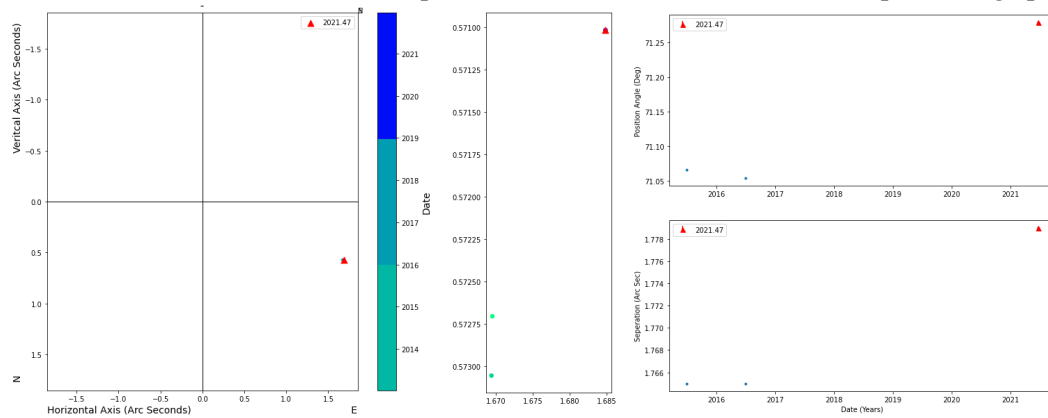


Figure 1: Images of each observation after bispectrum phase reconstruction. The green circle marks the primary star and the magenta circle marks the secondary star. Target number, date, and filter are included for each observation above the image. Separation and position angle for each observation are included below the image where we were able to resolve the image. Not pictured: Targets 7 and 8.

4. Discussion

4.1 Target 1

This system is not listed in the WDS. According to the EDR3 parallax data in the DPC, there is a 0% probability that A and B are within 1 light year of each other. When the DR2, EDR3, and our measurements are entered into the DSPT, we find our measurements do not closely conform to the measurements derived using Gaia celestial coordinates. Since the two stars are not likely gravitationally bound, the difference may be in the movement of the stars in space or due to limitations in the telescope or image processing.

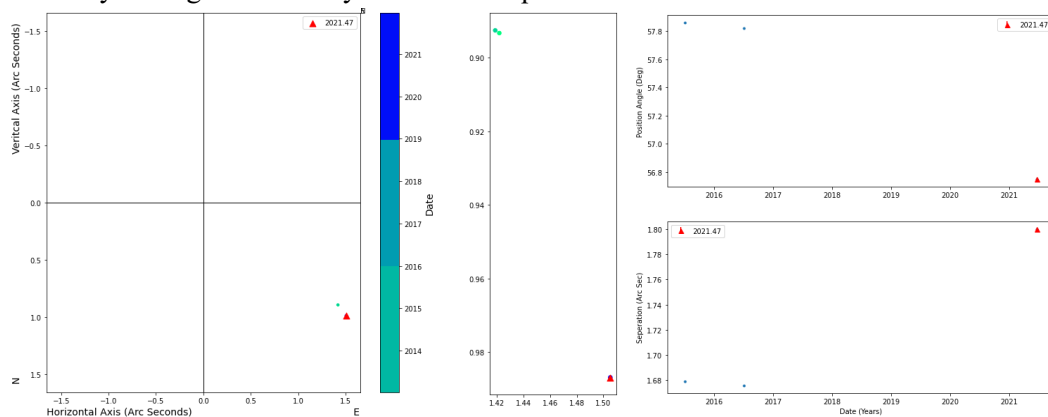


4.2 Target 2

This system is not listed in the WDS. According to the EDR3 data, there is a 0% probability that A and B are within 1 light year of each other. We were not able to obtain measurements of these stars.

4.3 Target 3

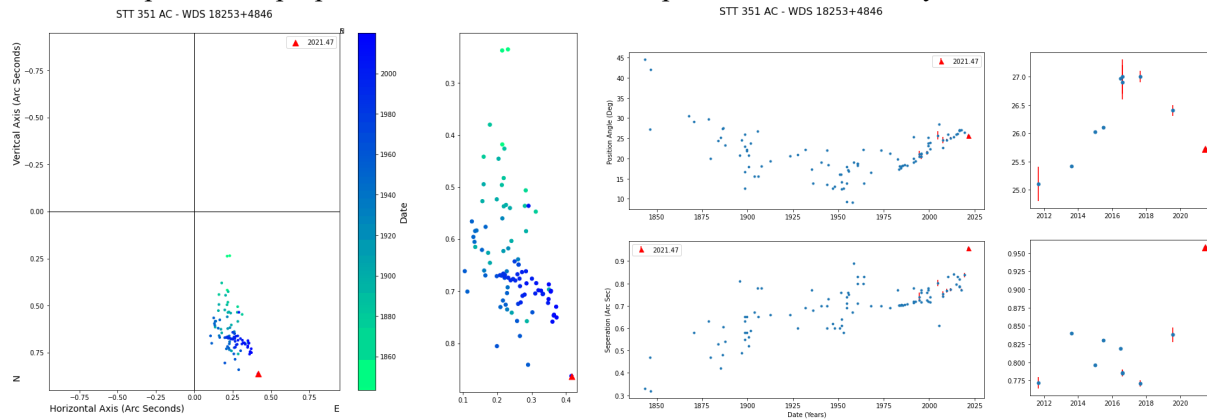
This system is not listed in the WDS. According to the DPC, there is a 94.2% probability the stars are within 1 light year of each other. When input into the DSPT, our measurements slightly differ from the results derived from the Gaia DR2 & EDR3 celestial coordinates. Based on the parallax analysis, these two stars are likely to be gravitationally bound but require further measurements to confirm.



4.4 Target 4

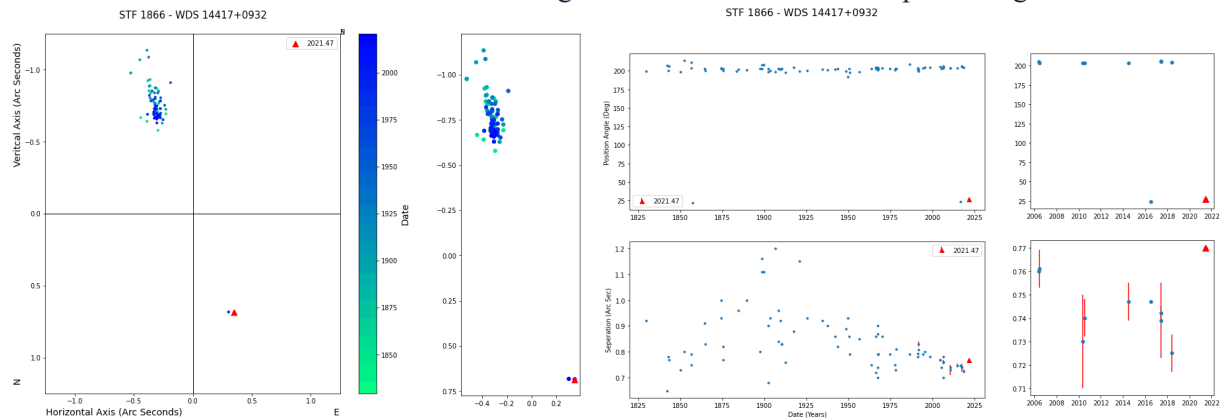
This system is in the WDS as 18253+4846, = STT 351 AC. The AB component is HU 66, which according to the WDS's last measurement in 2016 has magnitudes of 7.90/8.40, separation of 0.099", and position angle of 159.3 degrees. Both AB and AC have grade 4 orbital solutions in the Sixth Orbital Catalog (Mason,

et. al. 2021). The AB component could not be resolved in our images; however, the relative brightness of the B star might interfere with the centroid positioning in the Speckle Toolbox, which could throw off our measurements of the AC component. Indeed our measurements do not agree with the historical trend. There is no EDR3 parallax or proper motion data for the C component, so further analysis could not be conducted.



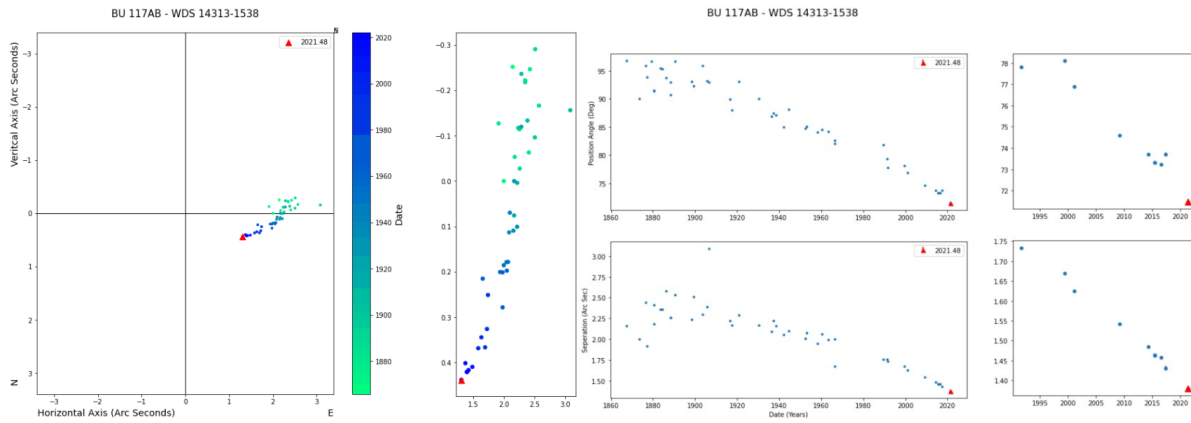
4.5 Target 5

This system is in the WDS as 14417+0932AB = STF1866 AB. There is a 1.9% probability the stars are within 1 light year of each other. As indicated in the DSPT graphs, our measurements significantly differ from the recent historical measurements and might indicate an instrument or processing limitations.



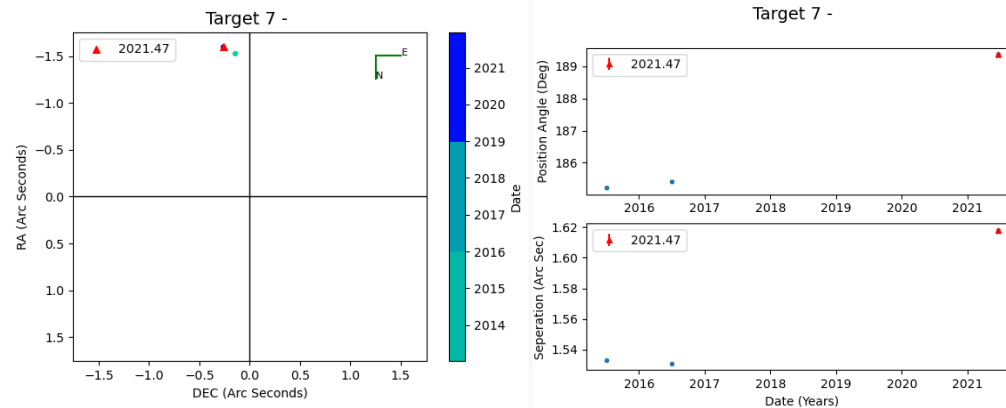
4.6 Target 6

This system is in the WDS as 14313-1538AB = BU 117AB, but it is uncertain if the system is physical. These stars have a 69.9% probability of being within 1 light year of each other. Our measurements agree nicely with the historical record, and when plotted present a parabolic curve around the primary star (focus), indicating a gravitationally bound system.



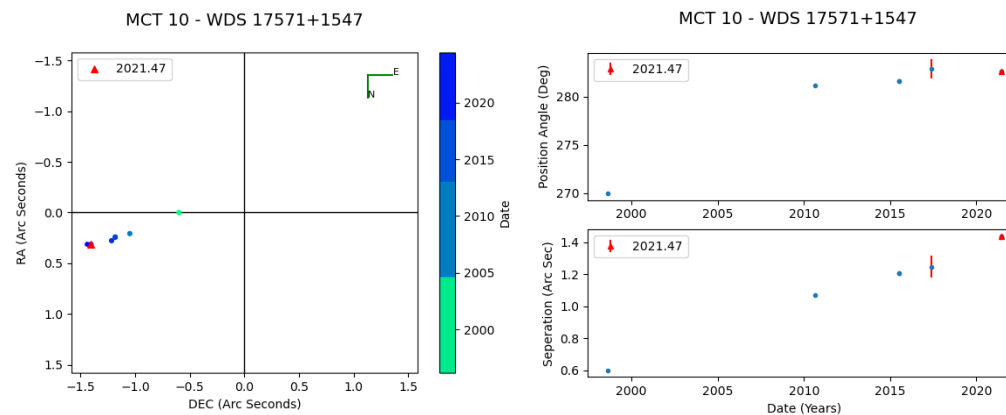
4.7 Target 7

This system is not listed in the WDS. According to the DPC, there is a 99.2% probability the stars are within 1 light year of each other. Based on parallax analysis, these two stars are likely to be gravitationally bound but require further measurements to confirm.



4.8 Target 8

This system is in the WDS as 17571+1547 = MCT 10, but it is uncertain if the system is physical. These stars have a 26.4% probability of being within 1 light year of each other. Our measurements fit in nicely with the historical record; however, the trend seems to be moving away from the origin.



5. Conclusion

Eight potential red dwarf binary systems were observed and then analyzed using speckle interferometry and bispectrum phase reconstruction to provide data used to infer whether the system is likely a physical or optical binary.

For targets 1, 3, and 7, there are only three data points for separation and position angle, and for target 2 there are only two. The data analyzed suggests that Targets 3 and 7 are gravitationally bound while Targets 1 and 2 are not. However, further observations are necessary to confirm these conclusions. Follow-up observations on Target 2 would benefit from using a telescope with a mirror diameter > 0.5 m due to the system's small separation angle and faintness. There already exists significant WDS data for Targets 4, 5, 6, and 8. Our measurements for Targets 4, 6, and 8 further suggest the systems are binary, but our measurement for Target 5 differs significantly from the historical record and therefore may not be reliable.

The sixteen individual observations across eight targets and two filters provide valuable data on the capabilities of BARO—and likely other telescopes with a mirror diameter of roughly 0.5 m—to provide photometric data on small-separation binary pairs. We conclude that BARO can observe binary pairs with $\rho > 1.5$ arcsec regardless of exposure time. With exposure times near 1 s, BARO likely cannot provide sufficient data for bispectrum phase reconstruction for pairs with $\rho < 1.5$ arcsec. For exposure times less than 50 ms, it is likely that BARO could provide sufficient observations for $\rho < 0.8$ arcsec.

Acknowledgments

We would like to acknowledge the Boyce Astro Robotic Observatory (BARO) for allowing us access to the remote telescope and Pat Boyce for assisting in observing. We would like to thank David Rowe for giving a presentation to our team on speckle interferometry and bispectrum phase reconstruction. We are grateful to Rick Wasson for giving our team a presentation on red dwarf stars. We also thank Russell Genet for addressing our team on methods of observing double stars. We thank Nathan Lehenbauer for the use of his Distance and Probability Calculator spreadsheet to help us analyze the parallax of the systems. Christine Filipek would like to acknowledge PlaneWave Instruments of Adrian, MI for their financial support of this project.

This research has made use of the Washington Double Star Catalog maintained at the U.S. Naval Observatory; we would like to thank Dr. Brian Mason and Dr. Rachel Matson for providing the WDS data used. This research has made use of data from the European Space Agency (ESA) mission Gaia (<https://www.cosmos.esa.int/gaia>), processed by the Gaia Data Processing and Analysis Consortium (DPAC, <https://www.cosmos.esa.int/web/gaia/dpac/consortium>). Funding for the DPAC has been provided by national institutions, in particular the institutions participating in the Gaia Multilateral Agreement. Extensive use of Stelle Doppie, (2020 December 25) version 2.7, a search engine for the WDS, was used <https://www.stelledoppie.it/index2.php?section=1> (accessed June-August 2021). Extensive use was made of VizieR, a search portal for astronomical databases maintained by Centre de Données astronomiques de Strasbourg, Gaia, <https://vizier.u-strasbg.fr/viz-bin/VizieR> (accessed June- August 2021).

References

- Dainty, J. C. (1975). Stellar Speckle Interferometry. *Topics in Applied Physics* (pp. 255–280). Springer Berlin Heidelberg. https://doi.org/10.1007/978-3-662-43205-1_7
- Dainty, J. C. (1981). Speckle interferometry in astronomy. *In Recent Advances in Observational*

- Astronomy* (pp. 95-109). <https://ui.adsabs.harvard.edu/abs/1981raoa.conf...95D>
Data Catalog, 2020, November, <https://ui.adsabs.harvard.edu/abs/2020yCat.1350....0G>, Provided by the
SAO/NASA Astrophysics Data System
- Edgeworth, K. E., 1946, *Nature*, 157(3989), 481–481. <https://doi.org/10.1038/157481d0>
- Gaia Collaboration. VizieR Online Data Catalog: Gaia EDR3 (Gaia Collaboration, 2020). VizieR
Online Data Catalog. <https://ui.adsabs.harvard.edu/abs/2020yCat.1350....0G>.
- Genet, R., Buchheim R., Johnson, J., Harshaw, R., & Freed, R. (2018). STAR Small Telescope
Astronomical Research Handbook (1st ed.). Tucson, AZ: Institute For Student Astronomical
Research (InStaR).
- Harshaw, R., Rowe, D., Genet, R., 2017, 13(1), 52-67
- Henry, T. J., Subasavage, J. P., Brown, M. A., Beaulieu, T. D., Jao, W.-C., & Hambly, N. C., 2004, *AJ*,
128(5), 2460-2473. <https://doi.org/10.1086/425052>
- Henry, T. J., Jao, W., Subasavage, J. P., Beaulieu, T. D., Ianna, P. A., Costa, E., & Méndez, R. A., 2006,
AJ 132(6), 2360–2371. <https://doi.org/10.1086/508233>
- Jiménez-Esteban, F. M., Solano, E., & Rodrigo, C., (2019), *AJ*, 157(2), 78.
<https://doi.org/10.3847/1538-3881/aafacc>
- Lada, C. J., 2006, *AJ*, 640(1), L63–L66. <https://doi.org/10.1086/503158>
- Mason, B. D., Wycoff, G. L. Hartkopf, W. I., Douglass, G. G., Worley C. E., 2001-2013, *AJ.*,
122, 3466. (B/wds/wds)
- Matson, R., Williams, S., Hartkopf, W., & Mason, B., (2021). Sixth Catalog of Orbits of Visual
Binary Stars, U.S. Naval Observatory, Washington, DC. <http://astro.gsu.edu/wds/orb6.html>
- Morgan, B. L., Beddoes, D. R., Scaddan, R. J., & Dainty, J. C., 1978, *MNRAS*, 183(4), 701-710.
<https://doi.org/10.1093/mnras/183.4.70>
- Petropulu, A. P., Nikias, C. L., 1992, *IEEE Trans. Signal Process.*, 40(3), 691-610.
<https://doi.org/10.1109/78.120803>
- Rowe, D. (2020). GAIA Double Star Selection Tool, version 1.02, GDS Notes.
[https://www.dropbox.com/sh/eowlk0q4u39c7do/AACw3uZcogaxiud79Fj70tr6a?dl=0&preview=
GDS+Notes.docx](https://www.dropbox.com/sh/eowlk0q4u39c7do/AACw3uZcogaxiud79Fj70tr6a?dl=0&preview=GDS+Notes.docx)
- Smolinsky, J., Osborn, W., 2006, *Rev. Mex. Astron. Astrofis*, 25. Bibcode:2006RMxAC..25...65S
Stelle Doppie. (2020, December 25). <https://www.stelledoppie.it/index2.php?section=1>
- United States Naval Observatory. (2010, October 2). Data from the Washington Double Star Catalog
(WDS). Washington D.C.
- Wasson, R., Rowe, D., & Genet, R., 2020, *JDSO*, 16-3, 208-228.